Versatile Fabrication of Ultralight Magnetic Foams and Application for Oil–Water Separation

Ning Chen and Qinmin Pan*

School of Chemical Engineering and Technology, Harbin Institute of Technology, Harbin 150001, People's Republic of China

ABSTRACT Ultralow-density (<10 mg cm^{-3}) materials have many important technological applications; however, most of them were fabricated using either expensive materials or complicated procedures. In this study, ultralight magnetic Fe_2O_3/C, Co/C, and Ni/C foams (with a density <5 mg cm^{-3}) were fabricated on the centimeter scale by pyrolyzing commercial polyurethane sponge grafted with polyelectrolyte layers based on the corresponding metal acrylate at 400 °C. The ultralight foams consisted of 3D interconnected hollow tubes that have a diameter of micrometer and nanoscale wall thickness, forming hierarchical structures from macroscopic to nanometer length scales. More interesting was that the wall thickness and morphology of the microtubes could be tuned by controlling the concentrations of acrylic acid and metallic cations. After modification with low-surface-energy polysiloxane, the ultralight foams showed superhydrophobicity and superoleophilicity, which quickly and selectively absorbed a variety of oils from a polluted water surface under magnetic field. The oil absorption capacity reached 100 times of the foams' own weight, exhibiting one of the highest values among existing absorptive counterparts. By controlling the composition and conformation of the grafted polyelectrolyte layers, the present approach is extendable to fabricate a variety of ultralow-density materials desirable for absorptive materials, electrode materials, catalyst supports, *etc.*

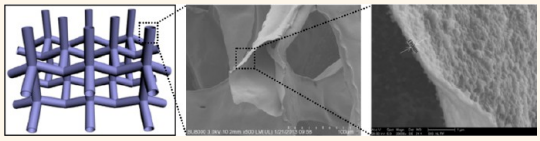

KEYWORDS: ultralight magnetic foams · polyelectrolyte-grafted PU sponge · 3D interconnected microtubes · hierarchical architecture · superhydrophobicity · oil–water separation

Ultralow-density (<10 mg cm^{-3}) materials have many important applications in the fields of sound and energy absorption, electrode materials, thermal management, and catalyst supports.[1,2] Until now, only a few existing materials show a density below 10 mg cm^{-3}, including silica aerogels (≥1.0 mg cm^{-3}),[3,4] carbon nanotube (CNT) sponges (5.8 mg cm^{-3}),[5] hybrid graphene/CNT foams (6.9 mg cm^{-3}),[6] CNT aerogels (4.0 mg cm^{-3}),[7] graphene foams (0.16–5.0 mg cm^{-3}),[8−11] nickel microlattices (0.9 mg cm^{-3}),[12] and aerographite (0.18 mg cm^{-3}).[13] However, most of these ultralight materials were fabricated using either expensive materials or complicated procedures, limiting their mass production and practical applications. In addition, except for metal microlattices,[12] all of the ultralight materials exhibit random cellular architectures and high surface area, which decrease some mechanical properties such as stiffness and strength. Therefore, it is important to explore a facile and versatile strategy capable of fabricating ultralight materials, as well as tailoring their properties and morphologies, but it remains a challenge.

From the standpoint of material design, building hierarchical structures (*e.g.*, from millimeter to micrometer and nanometer scales) is a crucial step for ultralight material synthesis.[12,14] In this regard, a commercial polyurethane (PU) sponge might be a desirable template for fabricating ultralight materials because it possesses millimeter-level pores and micrometer-scale interconnected skeletons.[15] But how to use a PU sponge as a versatile template for ultralight material synthesis has not been reported up to now. A main challenge is to construct a homogeneous, continuous, and mechanical robust nanostructure capable of forming a 3D porous hierarchical architecture at different length scales, as well as avoiding the collapse of the architecture after the removal of the sponge template.

Here, we reported a facile and versatile approach to fabricate ultralight magnetic foams using a commercial PU sponge as a

* Address correspondence to panqm@hit.edu.cn.

Received for review April 24, 2013 and accepted July 22, 2013.

Published online July 22, 2013
10.1021/nn4020533

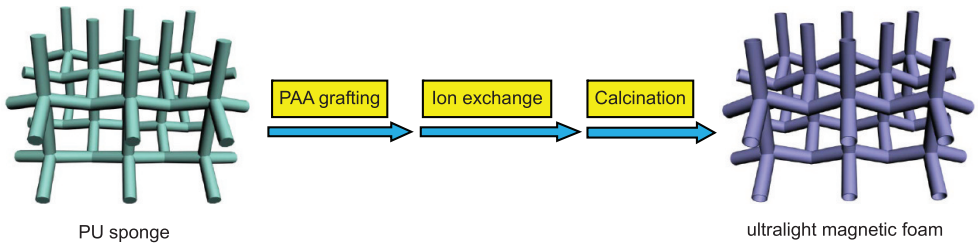

Scheme 1. Illustration of the fabrication of ultralight magnetic foams from a polyacrylic acid (PAA)-grafted polyurethane sponge. The foams were constructed from 3D interconnected microtubes having nanoscale wall thickness.

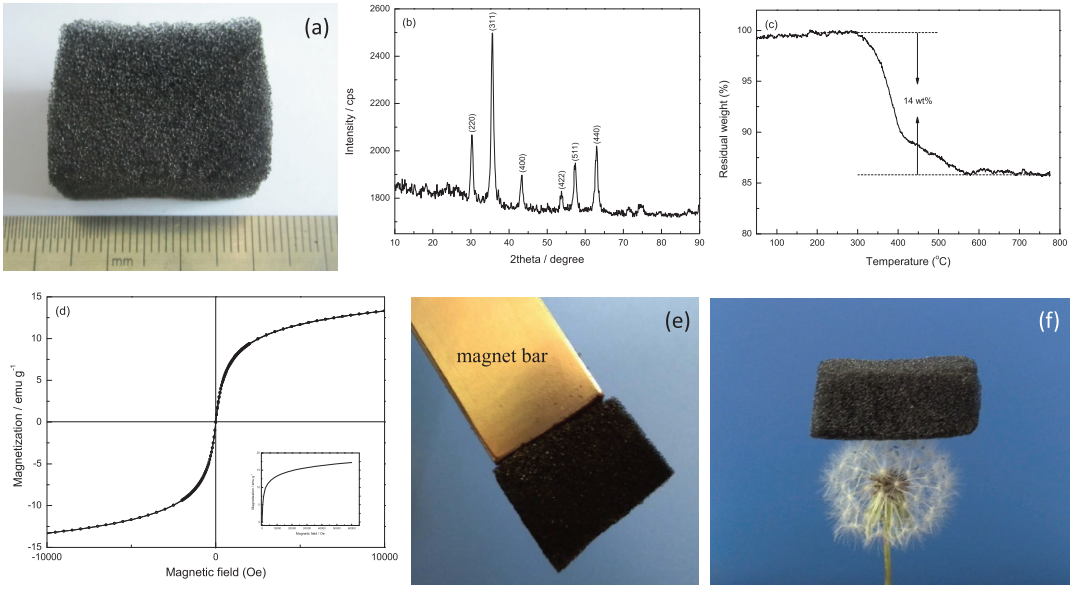

Figure 1. Optical image (a), XRD pattern (b), TG curve (c), and room-temperature magnetization hysteresis curve (d) of the as-prepared ultralight Fe_2O_3/C foams. The density of the foam is 3.9 mg cm^{-3}. A piece of ultralight Fe_2O_3/C foam could be manipulated by a magnet bar (e) and stand on a dandelion (f).

template for the first time. Monolithic ultralight Fe_2O_3/C, Co/C, and Ni/C foams were synthesized through the calcinations of the PU sponges grafted with corresponding poly(metal acrylate) layers at 400 °C (Scheme 1). The resulting foams exhibited hierarchical structures constructed by 3D interconnected microtubes that have a diameter of 40−50 μm and wall thickness of 190−300 nm, making them one of the lightest magnetic materials ever reported.[16−22] In this study, we successfully addressed the collapse challenge associated with 3D interconnected microtubes, as well as tuned the morphologies of the microtubes by elaborately controlling the composition and conformation of the grafted polyelectrolyte layers. Application of these novel ultralight foams was demonstrated by fast and selective removal of oils from a water surface under magnetic field. Although porous magnetic foams were fabricated in recent studies,[16−28] they rarely exhibited hierarchical structures built from 3D interconnected microtubes with controllable wall thickness and morphology. The densities of these foams were either not presented[23−28] or higher than tens of mg cm^{-3}.[16−22] Moreover, the application of superhydrophobic ultralight magnetic foams in oil−water separation was rarely investigated. With an elaborate choice and combination of polyelectrolyte layers and ions, this strategy might synthesize monolithic ultralight foams of varying constituents and properties.

RESULTS AND DISCUSSION

In order to obtain an ultralight magnetic material, we used a commercial polyurethane sponge as a template. At first, the surface of the PU sponge was homogeneously grafted with poly(acrylic acid) through cerium(IV) ammonium nitrate (CAN)-catalyzed polymerization,[29] as illustrated in Scheme 1. The presence of grafted poly(acrylic acid) was confirmed by XPS and contact angle measurements (Figure S1, Supporting Information). After cation exchange and coordination with Fe^{3+}, Ni^{2+}, and Co^{2+} as well as subsequent calcinations at 400 °C, monolithic magnetic foams at centimeter scale were obtained. Figure 1a shows a typical photograph of the as-prepared Fe_2O_3/C foams. They are completely black and still keep a sponge-like appearance (Figure S2a−S2c and Figures S4a−5Sa in the Supporting Information). A closer look reveals that these foams are constructed of a 3D interconnected network. The chemical compositions of the foams

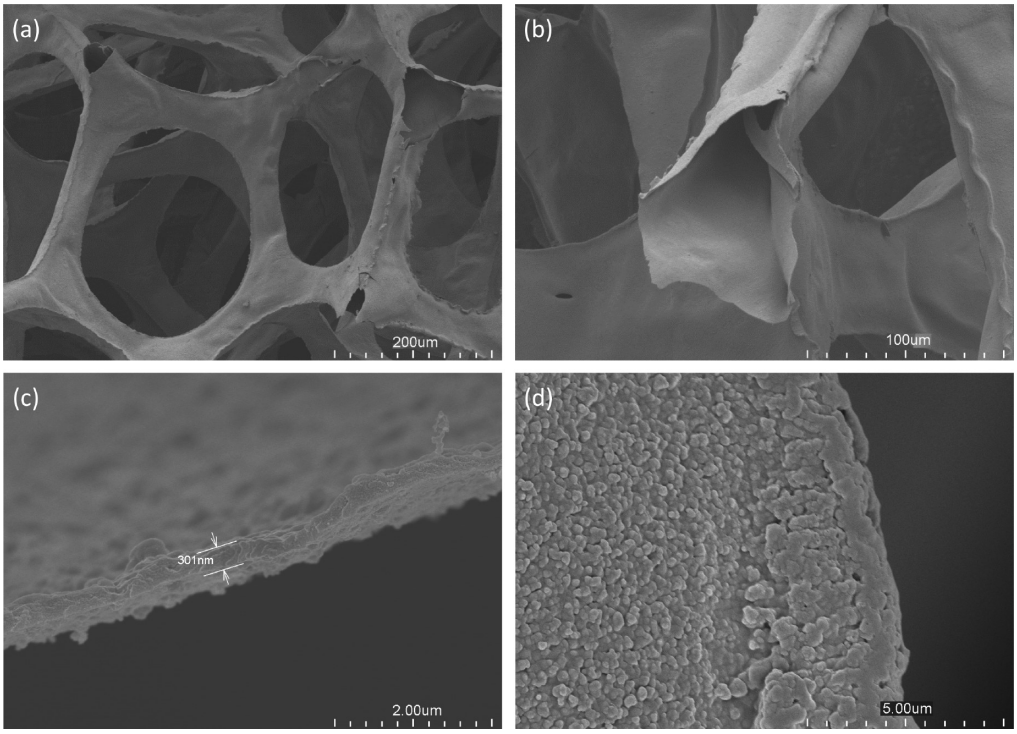

Figure 2. SEM images of the ultralight Fe_2O_3/C foams. (c) Cross-section image of a microtube. The concentrations of acrylic acid and $Fe(NO_3)_3$ for the foam synthesis were 1.0 wt % and 0.02 mol L^{-1}, respectively.

were identified by XRD measurements (Figure 1b and Figure S3a in the Supporting Information), confirming the presence of Fe_2O_3 and metallic Ni and Co phases as well as amorphous carbon. Notably, in the case of Fe_2O_3/C foams, calcinations at a temperature higher than 400 °C induced a phase change from Fe_2O_3 to Fe_3O_4 and Fe_3C. TGA measurements revealed that the foams contain 14−78 wt % amorphous carbon phase (Figure 1c and Figure S3b,3c in the Supporting Information). The magnetic properties of the ultralight foams were measured at room temperature. Fe_2O_3/C foams show superparamagnetism and have a saturation magnetization (M_s) of 17.2 emu g^{-1} (Figure 1d). Co/C and Ni/C foams exhibit weak ferromagnetic properties because they show coercive forces of 150.5 and 300.6 Oe as well as remanent magnetization of 0.03 and 0.95 emu g^{-1}, respectively (Figures S4d and S5d, Supporting Information). Therefore, the magnetic properties of the ultralight foams make them capable of being manipulated by a magnet bar (Figure 1e, Figures S4e and S5e, Supporting Information). The density of the foams was measured to be 3.9 (Fe_2O_3/C), 4.0 (Co/C), and 4.4 (Ni/C) mg cm^{-3}, which is comparable to the reported ultralight aerogels[1,3−5,13,30,31] but is about 10 times lower than those of other ultralight magnetic foams (Table S1, Supporting Information) including $Nd_2Fe_{14}B$-SiO_2 aerogels (140−200 mg cm^{-3}),[16] hybrid inorganic−organic magnetic foams (50−70 mg cm^{-3}),[17] and monolithic Ni-SiO_2, Fe_2O_3/Fe_3O_4−SiO_2, and Ni-Fe_2O_4−SiO_2 nanocomposites (50−60 mg cm^{-3}).[18] As a result, a piece of the ultralight Fe_2O_3/C foams could effortlessly stand on a dandelion (Figure 1f). The BET surface areas of the foams are 89.5 m^2 g^{-1} (Fe_2O_3/C), 83.4 m^2 g^{-1} (Co/C), and 93.4 m^2 g^{-1} (Ni/C), which are much less than those of ultralight aerogels having cellular architectures.[1,3−5,9,11,13] The above results demonstrate the possibility of fabricating ultralight magnetic foams by using a commercial PU sponge as a template.

The microstructures of these ultralight foams were investigated by scanning electron microscope (SEM) observations. SEM images in Figure 2a,b show that the foams are built from corrugated hollow microtubes to form a 3D interconnected architecture (also see Figures S4b and S5b, Supporting Information). Although the microtubes have a diameter of 40−50 μm, their wall thickness is only 200−300 nm (Figure 2c, Figures S4c and S5c, Supporting Information), forming hierarchy structures at both nanometer and micrometer scales. The surface of the microtubes has a roughness on the nanoscale (Figure 2d). As a result, the architecture of the foams can be divided into three levels of length scales, millimeter (pore), micrometer (hollow tube), and nanometer (hollow tube's wall), making them much lighter than other lightweight magnetic materials.[16−22] Further investigation on the microtubes by transmission electron microscopy (TEM) shows that they are composed of amorphous carbon and nanoparticles of a few tens of nanometers in grain size, forming a typical nanocomposite structure (Figure S6, Supporting Information).

It was revealed that the density of the Fe_2O_3/C foams could be tuned by simply controlling the amount of

grafted polyacrylic acid (PAA) and concentration of $Fe(NO_3)_3$. Table 1 shows the densities of the Fe_2O_3/C foams fabricated from different concentrations of acrylic acid and $Fe(NO_3)_3$. As expected, increasing acrylic acid content as well as $Fe(NO_3)_3$ concentration leads to a higher density. In comparison, the concentration of acrylic acid exerts a more significant impact on the density than that of $Fe(NO_3)_3$.

SEM observations show that the variation of the foams' density is related to the wall thickness of the interconnected microtubes. From the SEM images in Figure 2 and Figure 3a–c, one can find that the wall thickness of the microtubes decreases from 650 nm to 279 and 190 nm as the concentration of $Fe(NO_3)_3$ is lowered from 0.05 mol L^{-1} to 0.03 and 0.01 mol L^{-1}, respectively. Similar trends are also observed for the Fe_2O_3/C foams prepared from different concentrations of acrylic acid (Figure 3d–f). For example, the microtubes of the Fe_2O_3/C foams exhibit a thickness of 1.82 μm when the content of acrylic acid is 5.0 wt %, while the value is only 568 nm when the concentration decreases to 3.0 wt %, indicating that reducing AA concentration is beneficial for the formation of thinner walls. SEM images also indicate that AA concentration has a greater influence on the wall thickness of the microtubes compared with that of $Fe(NO_3)_3$.

TABLE 1. Effect of the Concentrations of Acrylic Acid (AA) and $Fe(NO_3)_3$ on the Density (mg cm^{-3}) of Fe_2O_3/C Foams

		concentration of $Fe(NO_3)_3$/mol L^{-1}				
		0.01	0.02	0.03	0.04	0.05
concentration of AA/wt %	1.0	3.3	3.9	4.2	6.6	6.6
	2.0	6.3	7.8	9.5	10.4	13.3
	3.0	8.3	8.0	8.4	10.7	13.6
	4.0	8.7	10.6	12.2	13.0	15.1
	5.0	16.8	18.7	17.7	25.5	32.0

However, collapse of the 3D interconnected microtubes occurred when the content of acrylic acid was decreased to 0.5 wt %. No monolithic foams but rather a powder-like solid was obtained in this case. More interestingly, SEM observations reveal that the morphologies of the microtubes can also be tuned by the concentration of acrylic acid. Figure S7 shows that the edges of the microtubes display a periodically wrinkled pattern as the acrylic acid concentration is increased to 4 and 5 wt %, forming a sharp contrast with those of the counterparts synthesized from low AA content (*e.g.*, 2 wt %). The wavelength of the surface wrinkles is on the order of micrometers. These results indicate the important role of the grafted poly(acrylic acid) in the morphology and density of the ultralight foams.

On the basis of the above results, a unique formation mechanism of the ultralight foams is proposed in Figure 4. In this study, the role of PU sponge is to act as the template for the formation of a 3D interconnected porous architecture, which means that the mechanical stability and morphology of the microtubes strongly depend on the thickness and microstructure of the grafted polyelectrolyte layer. Since a poly(acrylic acid) layer grafted to a sponge's skeleton is a kind of polyanionic brush containing carboxylic groups, its conformation and surface properties depend upon temperature and solution compositions such as pH, concentration, and type of salts.[32,33] In the absence of the metal nitrates, poly(acrylic acid) stretched its polymer chain away from sponge skeleton due to the electrostatic repulsion

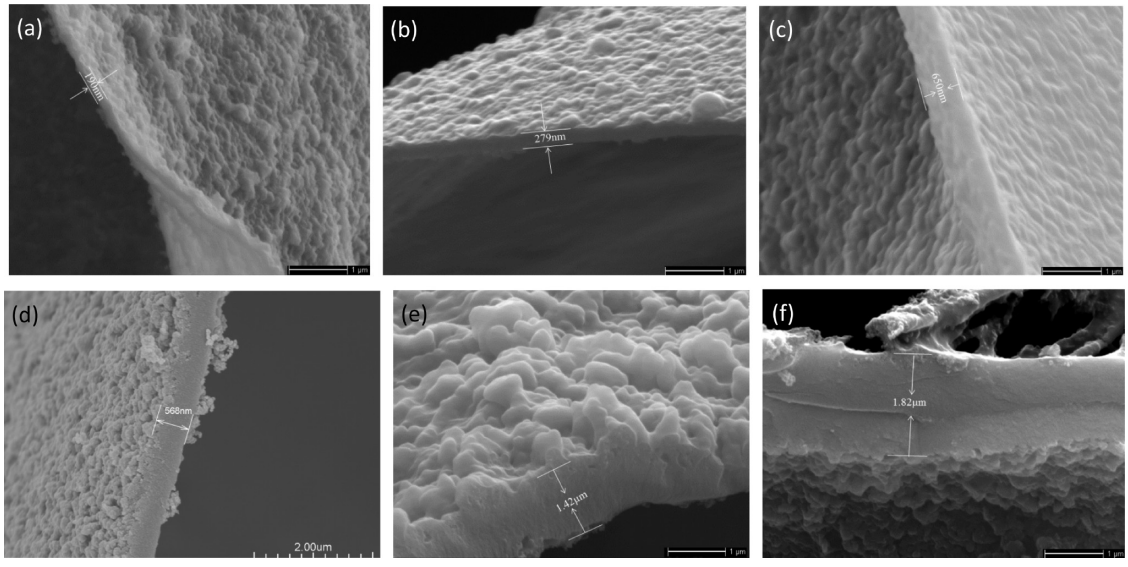

Figure 3. Effect of $Fe(NO_3)_3$ (a–c) and AA (d–f) concentrations on the wall thickness of the microtubes of Fe_2O_3/C foams. The concentrations of $Fe(NO_3)_3$ were (a) 0.01 mol L^{-1}, (b) 0.03 mol L^{-1}, and (c) 0.05 mol L^{-1}, and the concentration of AA was fixed at 1.0 wt %. The concentrations of AA were (d) 3.0 wt %, (e) 4.0 wt %, and (f) 5.0 wt %, and the concentration of $Fe(NO_3)_3$ was fixed at 0.02 mol L^{-1}.

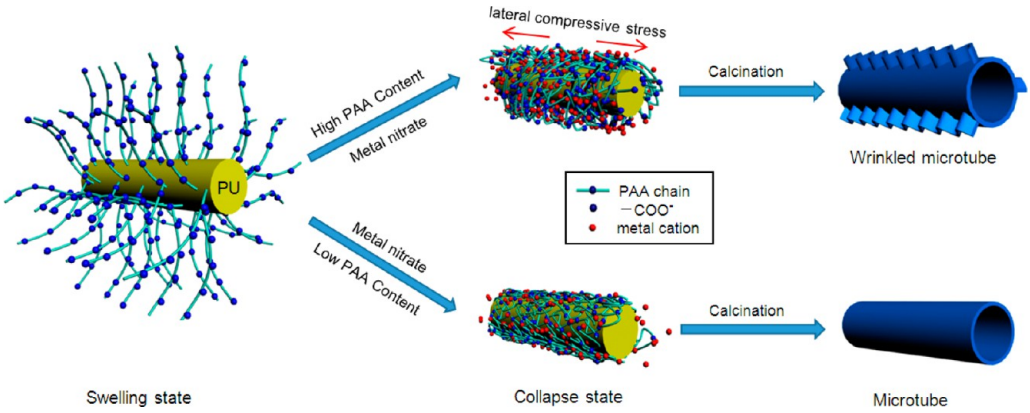

Figure 4. Schematic illustration for the formation mechanism of microtubes and surface wrinkles.

between adjacent negative-charged carboxyl groups, exhibiting a chain-expansion (or swelling) state.[34] Then the stretched polymer chain shrunk into a "collapsed state" as metal ions were added to the solutions due to the counterion screening effect,[35] leading to the condensation or enrichment of metal ions within the polymer layer. In the presence of polyvalent metal ions such as Fe^{3+}, the chain shrinkage was significant due to the strong charge neutralization caused by the coordination between the carboxylic group and the cations.[36] In this case, the carboxylic group of poly(acrylic acid) not only strongly attracted[37] but also coordinated with positively charged metal ions[36] when the grafted sponge was immersed in the aqueous nitrate solutions. After the cation exchange and coordination reactions, a relatively rigid poly(metal acrylate) layer was formed on the surface of the sponge. Then the polymeric precursor was converted to 3D porous foams where the basic structure is hollow microtubes after calcinations at 400 °C. Therefore, the mechanical stability of the interconnected microtubes depends on the thickness and integrity of their walls. For the grafted sponge prepared from high AA concentration, a sufficient poly(metal acrylate) layer was converted to form homogeneous, continuous, and mechanically robust microtubes, resulting in monolithic ultralight foams after the removal of the sponge template. On the contrary, no continuous and strong microtubes were formed to construct a mechanically stable 3D interconnected architecture when the acrylic acid content was lower than 0.5 wt %.

The formation of surface wrinkles is due to the fact that the poly(acrylic acid) layer is grafted to the sponge's skeleton. In the case of a high concentration of metal nitrate, more metal ions were captured by the carboxylic group of the PAA, forming a more rigid poly(metal acrylate) layer. Stress accumulation within the poly(metal acrylate) layer happened after the evaporation of water.[38] Because the poly(metal acrylate) layer was grafted to the underlying PU sponge, a lateral compressive stress was produced to counterbalance the layer expansion,[38] resulting in periodic wrinkles on the sponge's surface. The buckled polymeric layer was converted to the corresponding surface wrinkles in the subsequent calcination process. Because wrinkling behavior occurs only when the magnitude of the compressive stress exceeds a critical value for a thin rigid film tightly bound to a compliant underlying substrate,[39,40] the thickness of the grafted polymeric layer is a crucial factor for wrinkle formation. As a result, no wrinkled morphology was observed for the Fe_2O_3/C foams synthesized from low AA content. It should be noted that these wrinkled microtubes are beneficial for mechanically strengthening the foams. Therefore, the present results provide a simple and general strategy to control the constituents, morphology, and density of the ultralight foams by tuning the conformation and chemical composition of the grafted polyelectrolyte layer. Although the density and mechanical durability of the present foams are not as desirable as those of the reported graphene aerogel,[9−11] metallic microlattices,[12] and aerographite,[13] they still have the advantages of easy synthesis, low cost, and controllable microstructure. We believe that further improvements in the properties such as conductivity, stiffness, and chemical resistance will make the foams attractive multifunctional materials.

Application of Ultralight Foams for Oil−Water Separation. Application of these ultralight foams was investigated in the field of water−oil separation. In order to increase the selectivity of the foams for water−oil separation, the surface of the ultralight Fe_2O_3/C foams was changed to superhydrophobic (water-repellent) and superoleophilic (oil-absorbing) by treating with methyltrichlorosilane.[41] The contact angle of the modified foams for water and lubricating oil is 152° and 0°, respectively (Figure 5a,b). In fact, a flow of water bounced off the surface of the foams, and no water droplets were left on their surface after the siloxane modification. On the contrary, oils were rapidly absorbed by the foams in a few seconds, indicating that the modified foams can selectively separate oils from water. The selective absorption behaviors for oils and water are ascribed to the superhydrophobic and superoleophilic properties of the foams' surface, which originate from the hierarchically

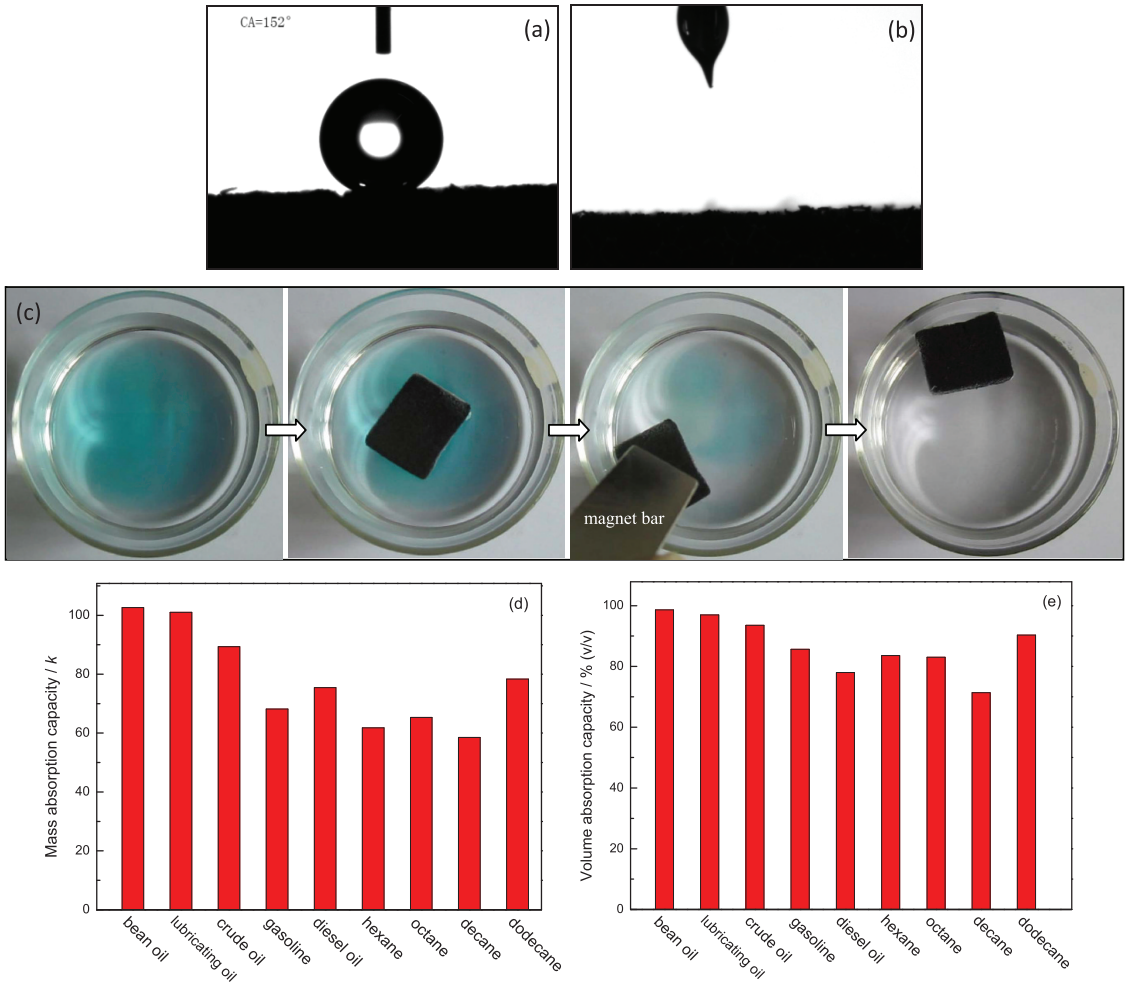

Figure 5. Contact angle of a water (a) and oil droplet (b) on the surface of the superhydrophobic Fe_2O_3/C foams. (c) Removal of lubricating oil from the surface of water by a piece of superhydrophobic foam under magnetic field; the lubricating oil was dyed blue to aid observation. Mass-based (d) and volume-based (e) absorption capacities of the superhydrophobic magnetic foams (with a density of 8.9 mg cm^{-3}) for oils and nonpolar solvents.

wrinkled structures coated on the microtubes,[42] as well as low-surface-energy polysiloxane coatings formed through the hydrolysis of methyltrichlorosilane.[41]

The modified foam absorbed a variety of oils including crude oil, bean oil, lubricating oil, and hexane more than 89.3, 102.6, 101, and 61.8 times its own weight, respectively, depending on density, viscosity, and surface tension of the absorbed liquids (Figure 5c,d). The oil-absorption capacities are much higher than other reported porous materials such as PU sponges (13−26 times),[42−44] organic nanocomposites (2−14 times),[45−48] 3D macroporous Fe/C (4−10 times),[49] graphene/α-FeOOH aerogel (12−27 times),[50] and nanocellulose aerogels (20−40 times),[51] but are close to spongy graphene (20−86 times),[52] carbon nanotube sponges (80−180 times),[5] and hybrid graphene/CNT foams (80−130 times),[6] indicating that the present foams exhibit one of the highest mass-absorption values. Since mass-based absorption capacity is strongly affected by the density of oils and absorbing materials,[51] we also used volume-based absorption capacity (V_{oil}/V_f) to characterize the absorptive capability of the ultralight foams. As shown in Figure 5e, the volume absorption capacities of the present foams for oils are higher than 71.3%, indicating that almost the whole volume of the foams is used for oil storage. These values are comparable to those of high-capacity carbonaceous materials such as CNT sponges (70−140% for hexane and 60−120% for chloroform),[5] nanocellulose aerogels (80% for hexane and 70% for chloroform),[51] and N-doped graphene frameworks (78.1% for gasoline),[9] but are higher than carbon ultralightweight aerogels (25.6% for crude oil and 5.9% for toluene).[11] Notably, carbon ultralightweight aerogels have a mass absorption capacity 200−600 times their weight. Therefore, although the present foams exhibit a lower mass-based capacity than their ultralight carbonaceous counterparts,[5,9,11] they still show one of the most efficient space utilizations for oil absorption.

The reason for the high oil-absorption capacity is that oils are mainly stored in the millimeter pores formed by the superoleophilic walls of the interconnected microtubes. Moreover, the interconnected microtubes also provide additional space for oil storage,

contributing to a high volume-based absorption capacity. Capillaries are believed to be the force driving the oils into the foams' bulk. The capillary flow is further strengthened by the superoleophilic interconnected microtubes when the oils spread into the inner pores of the foams, resulting in a high absorption capacity.[41,43] Interestingly, the foams could also be easily driven to the oil-polluted region by a magnet bar due to their magnetic properties, providing a facile and energy-saving method to collect oils from a polluted water area.[53] Therefore, the superhydrophobic magnetic foams display high oil-absorption capacity, high separation efficiency, and magnetic actuation. These interesting and important properties make the foams a kind of promising oil-absorbent material capable of quickly cleaning large-area oil spills. In addition, compared with the existing high-capacity absorptive materials such as graphene and CNT foams,[5,8−11] the present foams were fabricated through a simple procedure using commercially available materials, which is suitable for large-scale production.

CONCLUSIONS

In summary, we demonstrated a novel and general method for fabricating ultralow-density (down to 3.3 mg cm^{-3}) magnetic foams on the centimeter scale, as well as the oil−water separation properties of the foams. A unique structural characteristic of the foams is the 3D interconnected microtubes having a nanoscale wall thickness, making them one of the lightest magnetic materials ever reported.[16−22] Structural features of the foams (such as density, wall thickness, and morphology of microtubes) were dependent on the composition and conformation of the grafted polyelectrolyte layers, which could be simply tuned by controlling the concentrations of acrylic acid and metal nitrates. After being treated with methyltrichlorosilane, the resulting foams selectively adsorbed a wide range of oils and nonpolar solvents from the polluted water surface by a magnetic force and exhibited one of the highest oil-absorption capacities among the reported counterparts.[41−53] Because of the easy availability of raw materials and the simple fabrication process, the present finding offers a versatile strategy for the synthesis of ultralow-density foams that have potential applications as high-rate electrode materials, catalyst supports, thermal and acoustic insulation, templates for material synthesis, electromagnetic absorption, *etc*.

MATERIALS AND METHODS

Materials. Polyurethane sponges were supplied by Qingdao Yuquan Sponge Product Co., Ltd. (China). Potassium peroxydisulfate ($K_2S_2O_8$), cerium(IV) ammonium nitrate ($Ce(NH_4)_2(NO_3)_6$), nitric acid (HNO_3), acrylic acid (AA), iron(III) nitrate nonahydrate ($Fe(NO_3)_3\cdot 9H_2O$), cobalt nitrate hexahydrate ($Co(NO_3)_3\cdot 6H_2O$), and nickel nitrate hexahydrate ($Ni(NO_3)_3\cdot 6H_2O$) were purchased from Tianjin Kermel Chemical Reagent Co., Ltd. (China), and all were used as received.

Preparation of Ultralight Magnetic Foams. Polyurethane sponges (3 g) were cut into pieces of 2.5 cm × 2.0 cm × 1.5 cm in size, and then the sponge pieces were treated with 300 mL of a 10 wt % aqueous solution of $K_2S_2O_8$ for 5 h at 80 °C. The resulting sponges were rinsed with hot deionized water several times. The as-prepared sponges were put into a 400 mL aqueous solution containing 0.02 mol L^{-1} cerium(IV) ammonium nitrate, 0.2 mol L^{-1} nitric acid, and 1 wt % acrylic acid at 50 °C for 4 h in an Ar atmosphere; then the sponges were washed with 80 °C hot water for 24 h (the water was changed every 5 h) to remove homopolymer.

The modified sponges were dipped in 0.02 mol L^{-1} aqueous solutions of $Fe(NO_3)_3$, $Co(NO_3)_2$, and $Ni(NO_3)_2$, respectively. This process induced a cationic exchange reaction so that metal ions were strongly bound to carboxylic functionalities of poly(acrylic acid).[38] After being dried at room temperature, the resulting sponges were sintered at 400 °C for 1 h in an Ar atmosphere to obtain ultralight magnetic Fe_2O_3/C, Co/C, and Ni/C foams. A family of Fe_2O_3/C foams were fabricated by varying the concentrations of acrylic acid (1−5 wt %) and $Fe(NO_3)_3$ (0.01−0.05 mol L^{-1}). The density of the ultralight foams was calculated by the ratio of the weights to the geometric dimensions, which included the weight of entrapped air.

Preparation of Superhydrophobic Magnetic Foams. The obtained Fe_2O_3/C foams were dipped in a hexane solution of 2% (v/v) methyltrichlorosilane for 0.5 h and then dried at 80 °C for 12 h to prepare superhydrophobic magnetic foams.[36]

Characterizations of the Ultralight Magnetic Foams. The morphologies of the foams were observed using a FEI Quanta 200 scanning electron microscope. X-ray diffraction (XRD) analysis was performed on a Shimadzu XRD-6000. Transmission electron microscopy images were recorded on a Philips CM300 FEG. Brunauer−Emmett−Teller (BET) surface area of the foams was measured by using a Micromeritics ASAP 2020. Thermogravimetric analysis (TGA) was measured by a Netzsch STA-449F3 in air flow. X-ray photoelectron spectrum (XPS) measurement was conducted on a PHI-5700ESCA. The contact angles of the foams were measured by an OCA20 (Dataphysics Instruments). Magnetic properties of the ultralight foams were investigated on a magnetometer (Quantum Design MPMS XL).

Oil−Water Separation Experiments. Oils including lubrication oil, bean oil, and gasoline were dyed blue and then poured onto a water surface in a container. Superhydrophobic magnetic foams were put onto the surface of the water−oil mixtures. The oils were quickly absorbed into the open pores of the foams manipulated by a magnet bar. The oil-absorption capacity K of the foams was calculated by the ratio between the maximum absorbed oil quantity m_{oil} and the foams' mass m_f (*i.e.*, $K = m_{oil}/m_f$). Then the volume-based absorption capacity was given by the equation $V_{oil}/V_f = (m_{oil}\rho_f)/(m_f\rho_{oil})$,[46] where ρ_f and ρ_{oil} are the density of the magnetic foams and the oils, respectively.

Conflict of Interest: The authors declare no competing financial interest.

Supporting Information Available: XPS spectra and contact angles of the pristine and PAA-modified sponges, optical and SEM images of the pristine and PAA-modified sponges, XRD patterns and TG curves of the ultralight Co/C and Ni/C foams, optical and SEM images of the ultralight Co/C and Ni/C foams, TEM images of the ultralight Fe_2O_3/C, Co/C, and Ni/C foams, densities of the reported low-density magnetic foams, SEM images of the microtubes of the Fe_2O_3/C foams prepared from different concentrations of acrylic acid. This material is available free of charge *via* the Internet at http://pubs.acs.org.

Note Added after ASAP Publication. This manuscript posted ASAP on July 25, 2013. Panel C in Figure S1 of the Supporting Information file was replaced and the revised version was reposted on August 2, 2013.

REFERENCES AND NOTES

1. Hüsing, N.; Schubert, U. Aerogels-Airy Materials: Chemistry, Structure and Properties. *Angew. Chem., Int. Ed.* **1998**, *37*, 22–45.
2. Yoldas, B. E.; Annen, M. J.; Bostaph, J. Chemical Engineering of Aerogel Morphology Formed under Nonsupercritical Conditions for Thermal Insulation. *Chem. Mater.* **2000**, *12*, 2475–2484.
3. Tillotson, T. M.; Hrubesh, L. W. Transparent Ultralow-Density Silica Aerogels by a Two-Step Sol-Gel Process. *J. Non-Cryst. Solids* **1992**, *145*, 44–50.
4. Leventis, N.; Leventis, C. S.; Zhang, G. H.; Rawashdeh, A. M. Nanoengineering Strong Silica Aerogels. *Nano Lett.* **2002**, *2*, 957–960.
5. Gui, X.; We, J.; Wang, K.; Cao, A.; Zhu, H.; Jia, Y.; Shu, Q.; Wu, D. Carbon Nanotube Sponges. *Adv. Mater.* **2010**, *22*, 617–621.
6. Dong, X.; Chen, J.; Ma, Y.; Wang, J.; Chan-Park, M. B.; Liu, X.; Wang, L.; Huang, W.; Chen, P. Superhydrophobic and Superoleophilic Hybrid Foam of Graphene and Carbon Nanotube for Selective Removal of Oils or Organic Solvents from the Surface of Water. *Chem. Commun.* **2012**, *48*, 10660–10662.
7. Zou, J.; Liu, J.; Karakoti, A. S.; Kumar, A.; Joung, D.; Li, Q.; Khondaker, S. I.; Seal, S.; Zhai, L. Ultralight Multiwalled Carbon Nanotube Aerogel. *ACS Nano* **2010**, *4*, 7293–7302.
8. Chen, Z.; Ren, W.; Gao, L.; Liu, B.; Pei, S.; Cheng, H. M. Three-Dimensional Flexible and Conductive Interconnected Graphene Networks Grown by Chemical Vapor Deposition. *Nat. Mater.* **2011**, *10*, 424–428.
9. Zhao, Y.; Hu, C.; Hu, Y.; Cheng, H.; Shi, G.; Qu, L. A Versatile, Ultralight, Nitrogen-Doped Graphene Framework. *Angew. Chem., Int. Ed.* **2012**, *51*, 11371–11375.
10. Hu, H.; Zhao, Z.; Wan, W.; Gogotsi, Y.; Qiu, J. Ultralight and Highly Compressible Graphene Aerogels. *Adv. Mater.* **2013**, *25*, 2219–2223.
11. Sun, H.; Xu, Z.; Gao, C. Multifunctional, Ultra-Flyweight, Synergistically Assembled Carbon Aerogels. *Adv. Mater.* **2013**, *25*, 2554–2560.
12. Schaedler, T. A.; Jacobsen, A. J.; Torrents, A.; Sorensen, A. E.; Lian, J.; Greer, J. R.; Valdevit, L.; Carter, W. B. Ultralight Metallic Microlattices. *Science* **2011**, *334*, 962–965.
13. Mecklenburg, M.; Schuchardt, A.; Mishra, Y. K.; Kaps, S.; Adelung, R.; Lotnyk, A.; Kienle, L.; Schulte, K. Aerographite: Ultra Lightweight, Flexible Nanowall, Carbon Microtube Material with Outstanding Mechanical Performance. *Adv. Mater.* **2012**, *24*, 3486–3490.
14. Wilson, M. Building Ultralight Lattices. *Phys. Today* **2012**, *65*, 13.
15. Eaves, D. *Handbook of Polymer Foams*; Rapra Technology Limited, UK, 2004.
16. Gich, M.; Casas, L.; Roig, A.; Molins, E. High Coercivity Ultralight Transparent Magnets. *Appl. Phys. Lett.* **2003**, *82*, 4307–4309.
17. Ghosha, G.; Vilcheza, A.; Esquenaa, J.; Solansa, C.; Rodríguez-Abreu, C. Preparation of Ultra-Light Magnetic Nanocomposites Using Highly Concentrated Emulsions. *Mater. Chem. Phys.* **2011**, *130*, 786–793.
18. Popovici, M.; Gich, M.; Savii, C. Ultra-Light Sol-Gel Derived Magnetic, Nanostructured Materials. *Rom. Rep. Phys.* **2006**, *58*, 369–378.
19. Li, T.; Liu, H.; Zeng, L.; Yang, S.; Li, Z.; Zhang, J.; Zhou, X. Macroporous Magnetic Poly(Styrene-Divinylbenzene) Nanocomposites Prepared *via* Magnetite Nanoparticles-Stabilized High Internal Phase Emulsions. *J. Mater. Chem.* **2011**, *21*, 12865–12872.
20. Chen, W. F.; Li, S. R.; Chen, C. H.; Yan, L. F. Self-Assembly and Embedding of Nanoparticles by In Situ Reduced Graphene for Preparation of a 3D Graphene/Nanoparticle Aerogel. *Adv. Mater.* **2011**, *23*, 5679–5683.
21. Biasetto, L.; Francis, A.; Palade, P.; Principi, G.; Colombo, P. Polymer-Derived Microcellular SiOC Foams with Magnetic Functionality. *J. Mater. Sci.* **2008**, *43*, 4119–4126.
22. Liu, S.; Yan, Q.; Tao, D.; Yu, T.; Liu, X. Highly Flexible Magnetic Composite Aerogels Prepared by Using Cellulose Nanofibril Networks as Templates. *Carbohydr. Polym.* **2012**, *89*, 551–557.
23. Chmielus, M.; Zhang, X. X.; Witherspoon, C.; Dunand, D. C.; Müllner, P. Giant Magnetic-Field-Induced Strains in Polycrystalline Ni-Mn-Ga Foams. *Nat. Mater.* **2009**, *8*, 863–866.
24. Gao, D.; Yang, G.; Zhu, Z.; Zhang, J.; Yang, Z.; Zhang, Z.; Xue, D. One-Step Synthesis of Open-Cell Ni Foams by Annealing the Ni^{2+}-Based Precursor in Air. *J. Mater. Chem.* **2012**, *22*, 9462–9465.
25. Lee, S. S.; Riduan, S. N.; Erathodiyil, N.; Lim, J.; Cheong, J. L.; Cha, J.; Han, Y.; Ying, J. Y. Magnetic Nanoparticles Entrapped in Siliceous Mesocellular Foam: A New Catalyst Support. *Chem.—Eur. J.* **2012**, *18*, 7394–7403.
26. Lee, J.; Lee, D.; Oh, E.; Kim, J.; Kim, Y. P.; Jin, S.; Kim, H. S.; Hwang, Y.; Kwak, J. H.; Park, J. G.; Shin, C. H.; Kim, J.; Hyeon, T. Preparation of a Magnetically Switchable Bioelectrocatalytic System Employing Cross-Linked Enzyme Aggregates in Magnetic Mesocellular Carbon Foam. *Angew. Chem., Int. Ed.* **2005**, *44*, 7427–7432.
27. Chun, J.; Lee, H.; Lee, S. H.; Hong, S. W.; Lee, J.; Lee, C.; Lee, J. Magnetite/Mesocellular Carbon Foam as a Magnetically Recoverable Fenton Catalyst For Removal of Phenol and Arsenic. *Chemosphere* **2012**, *89*, 1230–1237.
28. Topal, U.; Bakan, H. I. Permanently Magnetic $BaFe_{12}O_{19}$ Foams: Synthesis and Characterization. *Mater. Chem. Phys.* **2010**, *123*, 121–124.
29. Viklund, C.; Svec, F.; Fréchet, J. M.; Irgum, K. Fast Ion-Exchange HPLC of Proteins Using Porous Poly(Glycidyl Methacrylate-co-Ethylenedimethacrylate) Monoliths Grafted with Poly(2-Acrylamido-2-Methyl-1-Propanesulfonic Acid). *Biotechnol. Prog.* **1997**, *13*, 597–600.
30. Pierre, A. C.; Pajonk, G. M. Chemistry of Aerogels and Their Applications. *Chem. Rev.* **2002**, *102*, 4243–4266.
31. Bryning, M. B.; Milkie, D. E.; Islam, M. F.; Hough, L. A.; Kikkawa, J. M.; Yodh, A. G. Carbon Nanotube Aerogels. *Adv. Mater.* **2007**, *19*, 661–664.
32. Zhou, F.; Hu, H.; Yu, B.; Osborne, V. L.; Huck, W. T. S.; Liu, W. Probing the Responsive Behavior of Polyelectrolyte Brushes Using Electrochemical Impedance Spectroscopy. *Anal. Chem.* **2007**, *79*, 176–182.
33. Drechsler, A.; Synytska, A.; Uhlmann, P.; Elmahdy, M. M.; Stamm, M.; Kremer, F. Interaction Forces between Micro-sized Silica Particles and Weak Polyelectrolyte Brushes at Varying pH and Salt Concentration. *Langmuir* **2010**, *26*, 6400–6410.
34. Misra, S.; Varanasi, S.; Varanasi, P. P. A Polyelectrolyte Brush Theory. *Macromolecules* **1989**, *22*, 4173–4179.
35. Ballauff, M.; Borisov, O. Polyelectrolyte Brushes. Current Opinion in Colloid & Interface. *Science* **2006**, *11*, 316–323.
36. Liu, Z.; Liu, J.; Hu, H.; Yu, B.; Chen, M.; Zhou, F. Reversible Hydration and Dehydration of Polyanionic Brushes Bearing Carboxylate, Phosphate and Sulfonate Side Groups: A Comparative AFM Study. *Phys. Chem. Chem. Phys.* **2008**, *10*, 7180–7185.
37. Wang, T. C.; Rubner, M. F.; Cohen, R. E. Polyelectrolyte Multilayer Nanoreactors for Preparing Silver Nanoparticle Composites: Controlling Metal Concentration and Nanoparticle Size. *Langmuir* **2002**, *18*, 3370–3375.
38. Kim, Y. H.; Lee, Y. M.; Lee, J. Y.; Ko, M. J.; Yoo, P. J. Hierarchical Nanoflake Surface Driven by Spontaneous Wrinkling of Polyelectrolyte/Metal Complexed Films. *ACS Nano* **2012**, *6*, 1082–1093.
39. Ebata, Y.; Crollb, A. B.; Crosby, A. J. Wrinkling and Strain Localizations in Polymer Thin Films. *Soft Matter* **2012**, *8*, 9086–9091.
40. Basu, S. K.; Bergstreser, A. M.; Francis, L. F.; Scriven, L. E.; McCormick, A. V. Wrinkling of a Two-Layer Polymeric Coating. *J. Appl. Phys.* **2005**, *98*, 063507.
41. Zhu, Q.; Chu, Y.; Wang, Z. K.; Chen, N.; Lin, L.; Liu, F. T.; Pan, Q. Robust Superhydrophobic Polyurethane Sponge as Highly Reusable Oil-Absorption Material. *J. Mater. Chem. A* **2013**, *1*, 5386–5393.
42. Yao, X.; Song, Y.; Jiang, L. Applications of Bio-Inspired Special Wettable Surfaces. *Adv. Mater.* **2011**, *23*, 719–734.

43. Calcagnile, P.; Fragouli, D.; Bayer, I. S.; Anyfantis, G. C.; Martiradonna, L.; Cozzoli, P. D.; Cingolani, R.; Athanassiou, A. Magnetically Driven Floating Foams for the Removal of Oil Contaminants from Water. *ACS Nano* **2012**, *6*, 5413–5419.
44. Zhu, Q.; Pan, Q.; Liu, F. Facile Removal and Collection of Oils from Water Surfaces through Superhydrophobic and Superoleophilic Sponges. *J. Phys. Chem. C* **2011**, *115*, 17464–17470.
45. Choi, S. J.; Kwon, T. H.; Im, H.; Moon, D. I.; Baek, D. J.; Seol, M. L.; Duarte, J. P.; Choi, Y. K. A Polydimethylsiloxane (PDMS) Sponge for the Selective Absorption of Oil from Water. *ACS Appl. Mater. Interfaces* **2011**, *3*, 4552–4556.
46. Hayase, G.; Kanamori, K.; Fukuchi, M.; Kaji, H.; Nakanishi, K. Facile Synthesis of Marshmallow-Like Macroporous Gels Usable under Harsh Conditions for the Separation of Oil and Water. *Angew. Chem., Int. Ed.* **2013**, *52*, 1–5.
47. Gupta, R.; Kulkarni, G. U. Removal of Organic Compounds from Water by Using a Gold Nanoparticle-Poly-(Dimethylsiloxane) Nanocomposite Foam. *ChemSusChem.* **2011**, *4*, 737–743.
48. Thanikaivelan, P.; Narayanan, T.; Pradhan, B. K.; Ajayan, P. M. Collagen Based Magnetic Nanocomposites for Oil Removal Applications. *Sci. Rep.* **2012**, *2*, 1–7.
49. Chu, Y.; Pan, Q. Three-Dimensionally Macroporous Fe/C Nanocomposites as Highly Selective Oil-Absorption Materials. *ACS Appl. Mater. Interfaces* **2012**, *4*, 2420–2425.
50. Cong, H. P.; Ren, X. C.; Wang, P.; Yu, S. H. Macroscopic Multifunctional Graphene-Based Hydrogels and Aerogels by a Metal Ion Induced Self-Assembly Process. *ACS Nano* **2012**, *6*, 2693–2703.
51. Juuso, T. K.; Marjo, K.; Robin, H. A. R.; Olli, I. Hydrophobic Nanocellulose Aerogels as Floating, Sustainable, Reusable, and Recyclable Oil Absorbents. *ACS Appl. Mater. Interfaces* **2011**, *3*, 1813–1816.
52. Bi, H.; Xie, X.; Yin, K.; Zhou, Y.; Wan, S.; He, L.; Xu, F.; Banhart, F.; Sun, L.; Ruoff, R. S. Spongy Graphene as a Highly Efficient and Recyclable Sorbent for Oils and Organic Solvents. *Adv. Funct. Mater.* **2012**, *22*, 4421–4425.
53. Zhu, Q.; Tao, F.; Pan, Q. Fast and Selective Removal of Oils from Water Surface *via* Highly Hydrophobic Core-Shell Fe_2O_3@C Nanoparticles under Magnetic Field. *ACS Appl. Mater. Interfaces* **2010**, *2*, 3141–3146.